한국공작기계학회 2002 추계학술대회 논문집 pp. 286~291

The Eclipse-II Parallel Mechanism for Motion Simulators

Jongwon Kim*, Jae Chul Hwang, Jin Sung Kim, Frank C. Park, and Young Man Cho

School of Mechanical and Aerospace Engineering
Seoul National University
San 56-1 Shinlim-dong Kwanak-gu, Seoul, Korea
**jongkim@snu.ac.kr*

Abstract: *We present the analysis and design of a new six degree-of-freedom parallel mechanism, Eclipse-II, which can be used as a basis for general motion simulators. This mechanism allows x, y and z-axis translations and a, b and c-axis rotations. Most significantly, it presents the advantage of enabling continuous 360 degrees spinning of the platform. We first describe the computational procedures for the forward and inverse kinematics of the Eclipse-II. Next, the complete singularity analysis is presented for the two cases of end-effector and actuator singularities. Two additional actuators are added to the original mechanism to eliminate both types of singularities within the workspace. Some practical aspects of the prototype development are introduced.*

1. Introduction

Motion simulators are virtual reality systems that assume the appearance of a real situation by using audio-visual effects and movements of a motion base. Such devices are used for many purposes, e.g., flight and driving simulators to name only a few. The former are used for pilot training by providing the pilot with motions that reflect the state of the aircraft while the later reproduce the actual driving conditions for vehicle design and human factors studies. Broadly speaking a motion simulator consists of an auditory system to generate sound, a visual system to display images, and a motion base system to generate movements as a result of motion cues.

Most current simulators have adopted the Stewart-Gough platform shown in Fig. 1, as the motion base [1, 2]. This platform is a six degree-of-freedom parallel mechanism that permits both translational and rotational motions. The platform can only tilt as much as ±20-30 degrees and large motions, as the 360 degrees platform overturn, are impossible. That is, the overturn motion of the aircraft or the 360 degrees spin of the roller coaster cannot be reproduced by the Stewart platform.

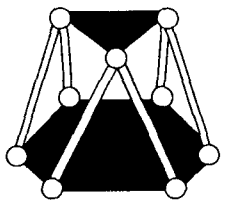

Fig. 1. Structure of Stewart-Gough platform

Some other parallel mechanisms that display relatively large translational or rotational motions are the Delta robot [3] and the spherical parallel mechanism [4]. Yet, the kinematic mobility of these mechanisms is not six and they are used either for positioning or orienting applications. Closer to the spirit of our design is the redundantly actuated Eclipse-I mechanism [5], devised specifically for machining applications. This mechanism has a large workspace and all closed trajectories on five faces of a cube can be traced without breaking contact. Though the spindle can rotate 360 degrees around the fixed z-axis and tilt concomitantly, the tilting angle of the upper plate does not exceed 90 degrees with respect to the vertical. Hence, large overturn motions are impossible and motion simulation applications restricted.

The objective of the present research is to develop a mechanism capable of 360 degrees tilting motion of the platform as well as translational motion. Fig. 2 shows the Eclipse-II mechanism and an example of its rotational motion capability. Since there are no limits in the rotational motion, it is possible to design a more realistic and higher fidelity motion simulator. This study emphasizes some of the practical aspects encountered when designing parallel mechanism and raises new and open research issues.

The paper is organized as follows. In Section 2, we describe the kinematic structure of the Eclipse-II, including the computational procedures for the forward and inverse kinematics. The singularity analysis and a method for eliminating the singularities are presented in Section 3. In Section 4, the prototype Eclipse-II, which is currently being built at Seoul National University is depicted. Finally some concluding remarks follow in Section 5.

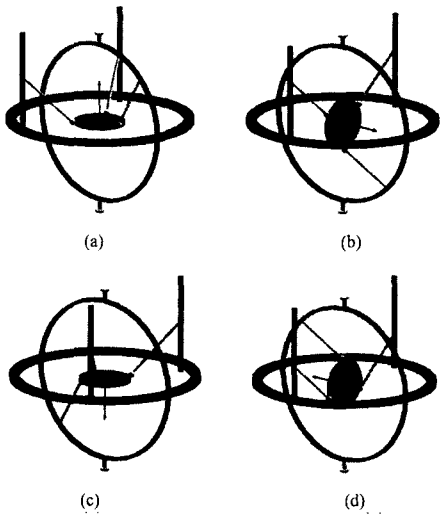

Fig. 2. Eclipse-II mechanism and its 360 degrees continuous rotational motions: (a) Rotation angle 0°, (b) Rotation angle 90°, (c) Rotation angle 180°, and (d) Rotation angle 270°.

2. Kinematics of the Eclipse-II

This section presents the architecture of the Eclipse II, followed by procedures describing the inverse and forward kinematics. As shown in Fig. 3, the Eclipse-II consists of three *PPRS* serial sub-chains that move independently on a fixed circular guide. Here, *P*, *R*, and *S* denote prismatic, revolute, and spherical joints, respectively. The Eclipse-II has six degrees-of-freedom and six actuated joints. These joints are the three *A* joints (*P*) along the horizontal circular guide, the C_2 and C_3 joints (*P*) on the vertical columns and another *P* joint (C_1) on the vertical circular column. All six actuated joints can be found in Fig. 3, and are indicated by arrows. The connecting links, C_iB_i, are attached to the circular and vertical columns respectively through revolute joints. The other ends of these links are mounted to the moving platform via three, points B_i on the figure, ball-and-socket joints. Mounting one circular column and two

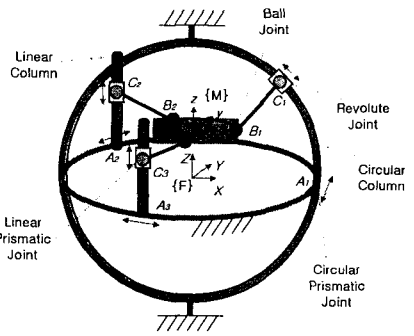

Fig. 3. Architecture of the Eclipse-II mechanism

linear columns on the circular guide results in the Eclipse-II having a large orientation workspace. Thus, the platform can rotate 360 degrees continuously about the *y*-axis in the moving frame $\{M\}$ (center of the moving platform) and the *Z*-axis in the fixed frame $\{F\}$ (center of the fixed horizontal track), respectively, as shown in Fig. 3. Coordinates and joint convention of the Eclipse-II are described in Fig. 4. The kinematic parameters of the mechanism are as follows: the fixed circular guide radius, r_a, the circular column radius, r_b, the radius of the moving platform, *r*, the length of the connecting C_iB_i links, L_i, and *d*, the distance between the spherical joints on the upper platform. The joint values are referred to as θ_{ij}, where *i* stands generally for the column index and *j* for the joint level (1 for the fixed circular guide, 2 for the circular and linear columns and 3 for the revolute joints on the same columns). For instance, θ_{32} refers to the prismatic joint on the third linear column.

2.1 Inverse Kinematics

The problem of inverse kinematics is to determine the values of the actuated joints from the position and orientation of the moving frame $\{M\}$ attached to the moving platform. For the Eclipse-II mechanism, the inverse kinematics can be solved by successively solving the inverse kinematics of each sub-chain. The algorithm

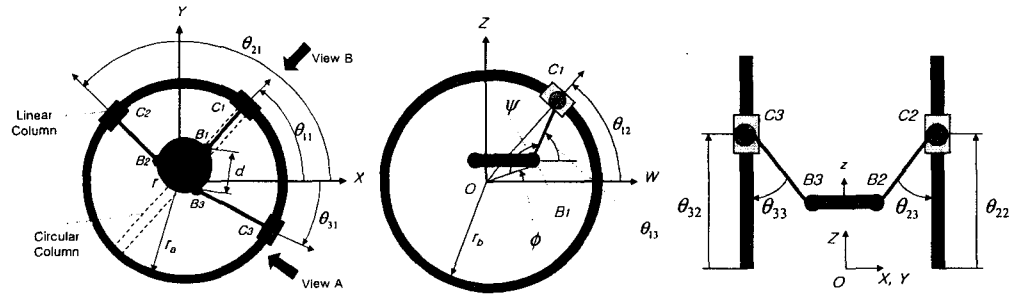

Fig. 4. Coordinate and joint convention: (a) Top view, (b) Side view A, and (c) Side view B

for solving the inverse kinematics is as follows:

1. Given the position $\vec{p}$ and orientation R of the moving platform in the fixed {F} frame, find the Cartesian position of the spherical joints:

$$\vec{b_i} = R\ {}^{M}\vec{b_i} + \vec{p} \tag{1}$$

where ${}^{M}\vec{b_i}$ is the vector of the i^{th} spherical joint expressed in the moving frame coordinate. R, $\vec{p}$, and $\vec{b_i}$ are all expressed in the fixed frame coordinates.

2. The circular prismatic joint values (A_i) are calculated from the positions of the spherical joints as follows:

$$\theta_{i1} = \arctan_2(b_{iy}, b_{ix}) \tag{2}$$

where θ_{i1} is the i^{th} circular prismatic joint value, and b_{ix} and b_{iy} are the x and y coordinates of $\vec{b_i}$, respectively.

3. Calculate the revolute joint value, θ_{13} (see Fig. 4b), on the vertical circular column:

$$\theta_{13} = 180° + \phi - \psi \tag{3}$$

where,

$$\phi = \arcsin\left(\frac{b_{1z}}{\left\|\vec{b_1}\right\|}\right),\quad \psi = \arccos\left(\frac{\left\|\vec{b_1}\right\|^2 + L_1^2 - r_b^2}{2\cdot\left\|\vec{b_1}\right\|\cdot L_1}\right),$$

and b_{iz} is the z coordinates of $\vec{b_i}$.

4. Determine the prismatic joint values, θ_{i2}, on the vertical circular column:

$$\theta_{i2} = \arctan_2(a_{iz}, a_{iw}) \tag{4}$$

where

$$a_{iz} = L_i\cos\theta_{i3} + \left\|\vec{b_1}\right\|\cos\phi,\quad a_{iw} = L_i\sin\theta_{i3} + \left\|\vec{b_1}\right\|\sin\phi.$$

5. Find the linear prismatic joint values, θ_{i2} (i = 2, 3), and the position of the revolute joints, θ_{i3} (i = 2, 3), on the vertical linear columns:

$$\theta_{i3} = \arccos\left(\frac{r_b - \sqrt{b_{ix}^2 + b_{iy}^2}}{L_i}\right), \tag{5}$$

$$\theta_{i2} = b_{iz} + L_i\sin\theta_{i3}. \tag{6}$$

Note that the solution of θ_{i3} is in the range [0°, 180°].

2.2 Forward Kinematics

The problem of forward kinematics is to determine the position and orientation of the moving frame given the actuated joint values. Similar to many other parallel mechanisms the forward kinematics solution is not unique and finding a closed form solution is a difficult task. If all of the actuated and passive joint values are known, the forward kinematics can be solved from the forward kinematics of each serial sub-chain. Therefore, the first step in the forward kinematics solution is to numerically determine the passive joint values from the actuated joint values by using the kinematics constraint equations.

The following algorithm solves iteratively the forward kinematic using the Newton-Raphson procedure:

1. The constraint equation between the active and passive joint values is generated from the condition that the distances between the ball-and-socket joints of the moving platform are constant:

$$\vec{g}(\vec{\theta}_a, \vec{\theta}_p) = \vec{0} \tag{7}$$

where,

$$\vec{g}(\vec{\theta}_a, \vec{\theta}_p) = \begin{bmatrix} (\vec{b_1} - \vec{b_2})\cdot(\vec{b_1} - \vec{b_2}) - d^2 \\ (\vec{b_2} - \vec{b_3})\cdot(\vec{b_2} - \vec{b_3}) - d^2 \\ (\vec{b_3} - \vec{b_1})\cdot(\vec{b_3} - \vec{b_1}) - d^2 \end{bmatrix}$$

$$\vec{b_i} = \begin{cases} \begin{bmatrix} \cos\theta_{i1}(r_a\cos\theta_{i2} - L_i\cos\theta_{i3}) \\ \sin\theta_{i1}(r_a\cos\theta_{i2} - L_i\cos\theta_{i3}) \\ r_a\sin\theta_{i2} - L_i\sin\theta_{i3} \end{bmatrix} & (i=1) \\ \begin{bmatrix} \cos\theta_{i1}(r_a - L_i\sin\theta_{i3}) \\ \sin\theta_{i1}(r_a - L_i\sin\theta_{i3}) \\ \theta_{i2} - L_i\cos\theta_{i3} \end{bmatrix} & (i=2,3) \end{cases} \tag{8}$$

$$\vec{\theta}_a = [\theta_{11}\quad \theta_{12}\quad \theta_{21}\quad \theta_{22}\quad \theta_{31}\quad \theta_{32}]^T$$

$$\vec{\theta}_p = [\theta_{13}\quad \theta_{23}\quad \theta_{33}]^T$$

2. Given the actuated joint values, find the passive joint ones for which the kinematic constraint equation (7) is satisfied. Because analytic differentiation of (7) is quite simple, a numerical approach like the Newton-Raphson method can be easily applied.

3. Determine the position and orientation of the moving frame from the forward kinematics equations for each sub-chain, equation (8), for the Cartesian coordinates of the spherical joints, and (9) and (10), from next section, for the position and orientation of the upper platform.

3. Singularity Analysis

Singularity refers to the configuration in which the number of degrees-of-freedom of the mechanism increases or reduces instantaneously. Since being close to one of the singularities can limit movement, disable control or break the mechanism, the singularity analysis is one of the most significant and critical problems in the design and control of parallel mechanisms.

Singularities of parallel mechanisms can be generally classified into two types: end-effector singularities and actuator singularities [5]. For the Eclipse-II mechanism, these two types of singularities co-exist in the workspace In this section, the singular configuration of the Eclipse-II mechanism and the method for eliminating singularities are described.

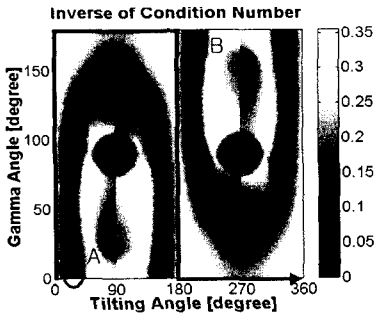

Fig. 5. Condition number plot of the actuator singularity configuration

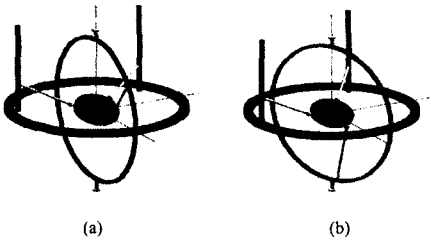

Fig. 6. Examples of the actuator singular configurations: (a) Point A in Fig. 5, (b) Point B in Fig. 5

The kinematic parameters used for singularity analysis are specified as follows. The radius of the circular guide (r_a), circular column (r_b) and moving platform (r) are, respectively, 1000 mm, 1000 mm, and 300 mm. The lengths of the connecting link in the circular column (L_1) and of the connecting links in the linear column (L_2, L_3) are, respectively, 900 mm and 870 mm.

3.1 Actuator Singularity

At an actuator singularity, the mechanism gains one or more degrees-of-freedom of possible motion, i.e., a self-motion occurs. Actuator singularity configurations can be determined from the Jacobian of the constraint equations. In the case of the Eclipse-II, the Jacobian of the constraint equation can be found by differentiating the constraint equation (7):

$$\frac{\partial g}{\partial \theta_a}\dot{\theta}_a + \frac{\partial g}{\partial \theta_p}\dot{\theta}_p = 0 \qquad (9)$$

where $\partial g / \partial \theta_p$ is a 3 × 3 matrix.

If the matrix $\partial g / \partial \theta_p$ is not of full rank, the passive joint values cannot be determined by the given active joint values, and then the mechanism is in one of the actuator singularity configurations.

Finding a closed form solution for the determinant roots (singularities) of the inverse of the Jacobian is a difficult task even when a specialized symbolic computational tool is available. Besides this once the roots have been identified a different and even more challenging task is establishing what roots are within the workspace of the mechanism, i.e., joint values are within admissible motion range and link interferences are avoided. Another possibility for identifying the singularities of a parallel mechanism lies in the use of line geometry and screw theory, that is particularly suited for symmetric parallel platforms connected by six serial structures, in which the number of actuators is equal to the kinematic degree of freedom of the platform. A different method, usually considered to be the simplest in the parallel mechanism literature, is to use a brute force algorithm and employ a numerical method that computes the condition number of the Jacobian at all points in the workspace. The condition number of Jacobian is defined as the ratio of the maximum singular value to the minimum singular.

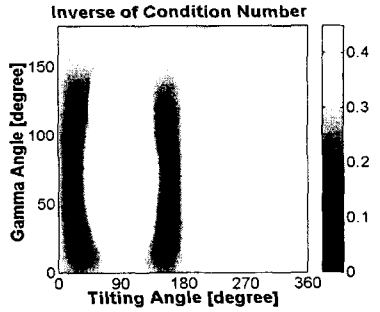

Fig. 7. Condition number plot of the actuator singularity configuration in the redundant case

Fig. 5 illustrates the condition number of $\partial g / \partial \theta_p$, while the platform tilts from 0° to 360°. The x-axis represents the tilting angle and the y-axis represents the rotation angle γ about the z-axis of the moving frame. As the condition number becomes larger, the mechanism moves nearer to an actuator singular configuration. For example, in the case of $\gamma = 0$, actuator singularities occur around tilting angles of 25° and 155°, the dark regions right above the tilting angle axis in the left side of the figure.

Fig.6 shows two examples (points A and B in Fig. 5) of actuator singular configurations of the Eclipse-II. In actuator singular configurations, two major problems exist. First, the platform cannot sustain its static equilibrium position in the presence of external force. In this case, the platform seems to have extra degrees of freedom. Second, the forward kinematic solutions are divided into two or more directions. Along the path crossing the actuator singular configuration, there exist multiple forward kinematic solutions with the same active joint values. Hence, there is a chance that the platform moves along an undesired direction.

One method for eliminating the actuator singular configurations is to redundantly actuate the mechanism by adding an actuator to one or more of the passive joints In the case of Eclipse-II, an additional actuator is added

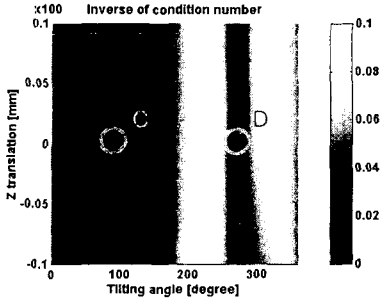

Fig. 8. Condition number plot of the end-effector singularity configuration

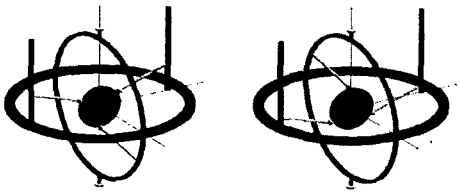

(a) (b)

Fig. 9. Examples of the end-effector singular configuration: (a) Point C in Fig. 8, (b) Point D in Fig. 8.

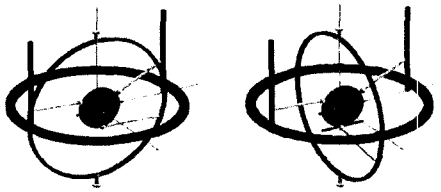

(a) (b)

Fig. 10. Y-direction motion of the Eclipse-II: (a) 6 d.o.f Eclipse-II and (b) 6+1 d.o.f Eclipse-II

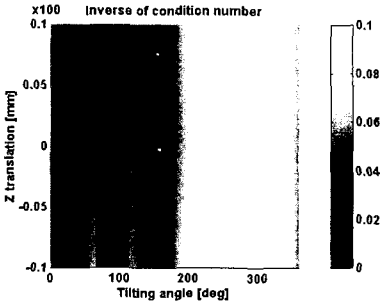

Fig. 11. Condition number plot of the end-effector singularity configuration of the 6+1 d.o.f Eclipse-II

to one revolute joint on one of the linear columns (thus $\partial g / \partial \theta_p$ reduces to a 3 × 2 matrix). Choosing one of the linear columns over the other one would only imply an upside-down turn of the figure. Comparing Fig. 7 with Fig. 5, it may be noted that the condition numbers reduced significantly and the majority of the actuator singular configurations are eliminated.

3.2 End-Effector Singularities

End-effector singularities are configurations in which the moving platform of the mechanism loses one or more degrees-of-freedom of possible motion. In this case the forward kinematic Jacobian loses rank. For Eclipse-II, the algorithm for solving the forward Jacobian is as follows:

1. The position of the moving platform $\vec{b}_c$ is the center of equilateral triangle determined by the three spherical joints.

$$\vec{b}_c = \frac{1}{3}(\vec{b}_1 + \vec{b}_2 + \vec{b}_3). \tag{10}$$

2. The rotational matrix representing the orientation of the moving platform is:

$$R = [R^x \quad R^y \quad R^z] \tag{11}$$

where,

$$R^x = \frac{1}{r}(\vec{b}_1 - \vec{b}_c),$$

$$R^y = \frac{1}{\sqrt{3}r}(\vec{b}_2 - \vec{b}_3),$$

$$R^z = R^x \times R^y.$$

3. In order to obtain the Jacobian matrix, equations (10) and (11) are differentiated:

$$\begin{bmatrix} v \\ w \end{bmatrix} = J\dot{\theta}, \quad J \in R^{6\times 9}. \tag{12}$$

Elements of the Jacobian, J, are as follows:

$$J_i = \left[\frac{1}{3}\left(\frac{\partial \vec{b}_i}{\partial \theta_i}\right)^T \quad R^z \cdot \frac{\partial R^y}{\partial \theta_i} \quad -R^z \cdot \frac{\partial R^x}{\partial \theta_i} \quad -R^x \cdot \frac{\partial R^y}{\partial \theta_i} \right]^T$$

($i = 1, 2, \cdots, 9$)

where, $\vec{b}_1 = \vec{b}_4 = \vec{b}_7$, $\vec{b}_2 = \vec{b}_5 = \vec{b}_8$, $\vec{b}_3 = \vec{b}_6 = \vec{b}_9$, $\theta_1 = \theta_{11}$, $\theta_2 = \theta_{21}$, $\theta_3 = \theta_{31}$, $\theta_4 = \theta_{12}$, $\theta_5 = \theta_{22}$, $\theta_6 = \theta_{32}$, $\theta_7 = \theta_{13}$, $\theta_8 = \theta_{23}$, $\theta_9 = \theta_{33}$.

4. Equation (12) can be expressed as

$$\begin{bmatrix} v \\ w \end{bmatrix} = J_a\dot{\theta}_a + J_p\dot{\theta}_p. \tag{13}$$

From equations (9) and (13), the relationship between the active joint velocity vector and the moving platform velocity vector can be expressed as

$$\begin{bmatrix} v \\ w \end{bmatrix} = J_f\dot{\theta}_a, \quad J_f \in R^{6\times 6} \tag{14}$$

where, $J_f = J_a - J_p\left(\frac{\partial g}{\partial \theta_p}\right)^{-1}\frac{\partial g}{\partial \theta_a}$.

Like the actuator singularities, end-effector singularities are established from the condition number

of the forward kinematic Jacobian at all points in the workspace.

The results in Fig. 8 are based on this numerical method, and illustrate the condition number of the forward Jacobian, while Eclipse-II tilts from 0° to 360°. The x-axis and y-axis in Fig. 8 represent the tilting angle and translation along Z-axis in the fixed frame, respectively. The dark regions around 90° and 270° in the figure represent the singular configurations of J_f, which in-effect are end-effector singularities.

Fig. 9 shows two examples of the end-effector singular configurations of the Eclipse-II. The end-effector singular configurations occur in positions where, with the platform tilted at 90° or 270°, one of the spherical joints is located on the Z-axis of the fixed frame. If the platform reaches one of the end-effector singular configurations of the Eclipse-II, there exist infinite solutions for the inverse kinematics. With other words there exist infinite possible sets of active joint values for one specific end-effector configuration of the moving platform. Even if it is possible to select only one solution of the inverse kinematics while the platform tilts from 0° to 360°, either the joints have infinite velocity or one linear column and the circular column collide with each other. As a solution to this problem, it is possible to change the solution of the inverse kinematics at an end-effector singular configuration while avoiding columns or roads collisions.

However, there still remains a problem, as shown in Fig. 10(a). At this configuration, the platform cannot translate along the y-direction in the moving frame Therefore, an actuator is added to change the position of the spherical joint that is connected to the circular column; that is, one degree-of-freedom is added to the original Eclipse-II. With this addition, the platform can now move along the y-direction at an end-effector singular configuration by changing the position of the spherical joint along the linear guide, whereas it is not necessary for the circular column to move [see Fig. 10(b)]. The additional actuator results in the elimination of the end-effector singularity within the workspace of the mechanism. Fig. 11 shows that the condition number of the forward kinematics Jacobian (now $J_f \in R^{6\times7}$) of Eclipse-II with the extra degree-of-freedom reduces significantly from that one corresponding to Fig. 8, at the tilting angles of 90° and 270°.

4. Development of the Prototype Eclipse-II

An experimental prototype actuated by servomotors is currently being developed to verify the motion performances of Eclipse-II architecture as a motion simulator. Table 1 describes specifications of the prototype. The structure consists of a fixed circular guide of radius of 200 mm, one circular column of the same radius and two vertical columns. Fixed roads, of lengths of 140 mm for the circular column and 178 mm for the other linear columns, are attached to the carriages using revolute joints. The connection to the upper platform is realized through spherical joints with angle limits of ±45 degrees. The spherical joints connect the tips of an isosceles triangle of base and height of 96 mm and 114 mm, respectively. The shape of the workspace is a cylinder of diameter and height of 52mm and 88 mm, respectively.

Table 1. Specifications of the prototype

Linear velocity	12m/min
Linear acceleration	0.1g
Rotational velocity	120deg/s
Rotational acceleration	500deg/s^2
Radius of circular guide	200mm
Rotational limit of spherical joint	±45deg
Workspace size	Ø52 x 88 mm

5. Conclusions

This paper deals with the analysis and design of a new redundant parallel mechanism, the Eclipse-II. The unique feature of this mechanism is that continuous 360 degrees rotational motion of the platform is possible in addition to the translational motion. Results for the forward and inverse kinematics, and the singular configuration analysis are presented. The original Eclipse-II mechanism shows both end-effector and actuator singular configurations within its workspace. Hence, a linear guide, where one spherical joint moves, is added to the mechanism to eliminate the end-effector singularity. An actuator is also added to one of two passive revolute joints on the vertical columns to eliminate the actuator singularities. For full tilting and turning motions the mechanism display good manipulability and a singularity-free workspace. Currently, a prototype is being build at Seoul National University. Preliminary calculations indicate a maximum velocity of the platform of 12 m/min. and an acceleration of 0.1 g.

Acknowledgements

This research was supported in part by the National Research Laboratory on Innovative Parallel Mechanism Platforms, and by the Brain Korea 21 program, both at Seoul National University.

References

[1] D. Stewart, "A Platform with six degrees of freedom," *Proc. Inst. Mech. Eng.*, Vol. 180, Part I, No.15, pp.371-386, 1966.

[2] G. P. Bertollini, et al., "The General Motors Driving Simulator," *SAE Paper 940179*, 1994.

[3] R. Clavel, "Conception d'un robot parallèle rapide à 4 degrés de liberté," *Ph.D. Thesis*, EPFL, Lausanne, No. 925, 1991.

[4] C. M. Gosselin, E. St-Pierre, "Development and Experimentation of a Fast 3-DOF Camera-Orienting Device," *The Int. J. of Robotics Research*, Vol. 16, No. 5, pp. 619-630, October, 1997.

[5] J. Kim, F. C. Park, S. Ryu, J. Kim, J. C. Hwang, C. Park, C. Iurascu, "Design and Analysis of a Redundantly Actuated Parallel Mechanism for Rapid Machining," *IEEE Transactions on Robotics and Automation*, Vol. 17, No. 4, pp. 423-434, 2001.